

2007

# Polarization Energy Gradients in Combined Quantum Mechanics, Effective Fragment Potential, and Polarizable Continuum Model Calculations

Hui li

*Iowa State University*

Mark S. Gordon

*Iowa State University, mgordon@iastate.edu*

Follow this and additional works at: [http://lib.dr.iastate.edu/chem\\_pubs](http://lib.dr.iastate.edu/chem_pubs)

 Part of the [Chemistry Commons](#)

The complete bibliographic information for this item can be found at [http://lib.dr.iastate.edu/chem\\_pubs/488](http://lib.dr.iastate.edu/chem_pubs/488). For information on how to cite this item, please visit <http://lib.dr.iastate.edu/howtocite.html>.

---

This Article is brought to you for free and open access by the Chemistry at Iowa State University Digital Repository. It has been accepted for inclusion in Chemistry Publications by an authorized administrator of Iowa State University Digital Repository. For more information, please contact [digirep@iastate.edu](mailto:digirep@iastate.edu).

---

# Polarization Energy Gradients in Combined Quantum Mechanics, Effective Fragment Potential, and Polarizable Continuum Model Calculations

## Abstract

A method that combines quantum mechanics (QM), typically a solute, the effective fragment potential (EFP) discrete solvent model, and the polarizable continuum model is described. The EFP induced dipoles and polarizable continuum model (PCM) induced surface charges are determined in a self-consistent fashion. The gradients of these two energies with respect to molecular coordinate changes are derived and implemented. In general, the gradients can be formulated as simple electrostatic forces and torques among the QM nuclei, electrons, EFP static multipoles, induced dipoles, and PCM induced charges. Molecular geometry optimizations can be performed efficiently with these gradients. The formulas derived for EFP/PCM can be generally applied to other combined molecular mechanics and continuum methods that employ induced dipoles and charges.

## Keywords

Double layers, Surface charge, Polarization, Electrostatics, Polarizability

## Disciplines

Chemistry

## Comments

The following article appeared in *Journal of Chemical Physics* 126 (2007): 124112, and may be found at doi:[10.1063/1.2711199](https://doi.org/10.1063/1.2711199).

## Rights

Copyright 2007 American Institute of Physics. This article may be downloaded for personal use only. Any other use requires prior permission of the author and the American Institute of Physics.

## Polarization energy gradients in combined quantum mechanics, effective fragment potential, and polarizable continuum model calculations

Hui Li and Mark S. Gordon

Citation: *The Journal of Chemical Physics* **126**, 124112 (2007); doi: 10.1063/1.2711199

View online: <http://dx.doi.org/10.1063/1.2711199>

View Table of Contents: <http://scitation.aip.org/content/aip/journal/jcp/126/12?ver=pdfcov>

Published by the [AIP Publishing](#)

---

### Articles you may be interested in

[United polarizable multipole water model for molecular mechanics simulation](#)

*J. Chem. Phys.* **143**, 014504 (2015); 10.1063/1.4923338

[An improved fragment-based quantum mechanical method for calculation of electrostatic solvation energy of proteins](#)

*J. Chem. Phys.* **139**, 214104 (2013); 10.1063/1.4833678

[Analytic energy gradients in combined second order Møller-Plesset perturbation theory and conductorlike polarizable continuum model calculation](#)

*J. Chem. Phys.* **135**, 144107 (2011); 10.1063/1.3649947

[Combining ab initio quantum mechanics with a dipole-field model to describe acid dissociation reactions in water: First-principles free energy and entropy calculations](#)

*J. Chem. Phys.* **132**, 074112 (2010); 10.1063/1.3317398

[Gradients of the polarization energy in the effective fragment potential method](#)

*J. Chem. Phys.* **125**, 194103 (2006); 10.1063/1.2378767

---

 **AIP** | APL Photonics

*APL Photonics* is pleased to announce  
**Benjamin Eggleton** as its Editor-in-Chief



# Polarization energy gradients in combined quantum mechanics, effective fragment potential, and polarizable continuum model calculations

Hui Li and Mark S. Gordon<sup>a)</sup>*Department of Chemistry, Iowa State University, Ames, Iowa 50011*

(Received 28 September 2006; accepted 31 January 2007; published online 30 March 2007)

A method that combines quantum mechanics (QM), typically a solute, the effective fragment potential (EFP) discrete solvent model, and the polarizable continuum model is described. The EFP induced dipoles and polarizable continuum model (PCM) induced surface charges are determined in a self-consistent fashion. The gradients of these two energies with respect to molecular coordinate changes are derived and implemented. In general, the gradients can be formulated as simple electrostatic forces and torques among the QM nuclei, electrons, EFP static multipoles, induced dipoles, and PCM induced charges. Molecular geometry optimizations can be performed efficiently with these gradients. The formulas derived for EFP/PCM can be generally applied to other combined molecular mechanics and continuum methods that employ induced dipoles and charges. © 2007 American Institute of Physics. [DOI: 10.1063/1.2711199]

## I. INTRODUCTION

Combined quantum mechanics and molecular mechanics (QM/MM) methods<sup>1,2</sup> are popular in theoretical modeling of many chemical systems. Dipole polarizability points (induced dipoles)<sup>3,4</sup> are often included in modern force fields to describe the polarization of the molecules represented by the force fields. It is also common to incorporate low-cost continuum solvation models<sup>5,6</sup> into the QM/MM calculations to assess bulk solvent effects with induced charges.

The effective fragment potential (EFP) is an *ab initio* based molecular mechanics method in which the molecular interaction parameters are obtained from preparative *ab initio* calculations.<sup>7</sup> The EFP is a polarizable method in which dipole polarizability tensors of the localized molecular orbitals (LMOs) are used<sup>8</sup> to calculate the EFP polarization energy from the induced dipoles. The polarizable continuum models (PCM), including the earlier dielectric PCM (D-PCM) (Ref. 9) and the more recent integration equation formalism (IEF)-PCM (Ref. 10), and conductorlike PCM (C-PCM) (Ref. 11), are continuum solvation models in which the solvent effects are described with induced apparent surface charges (ASCs). The bulk polarization energy can be calculated from the induced surface charges. The QM/EFP/PCM method<sup>12</sup> developed recently is a combined QM/MM/continuum method in which the EFP induced dipoles and PCM charges are iterated to self-consistency as the QM wave function converges.

Analytic energy gradients are important for efficient molecular geometry optimization and Hessian vibrational analysis. In this study the gradients of the EFP polarization energy and PCM solvation energy for combined QM/EFP/PCM and EFP/PCM calculations are derived and implemented.

This paper is organized as follows. In Secs. II A and II B, the EFP polarization energy and gradients and the

C-PCM solvation energy and gradients, respectively, are reviewed. In Sec. II C, the polarization and solvation energy/gradients in combined EFP/PCM calculations are derived. In Secs. II D and II E, the PCM related translational and rotational gradients in EFP/PCM calculations are derived and discussed in detail. Some numerical results are presented in Sec. III and conclusions are given in Sec. IV.

## II. THEORY

### A. EFP polarization

In the EFP method the intermolecular electrostatic interaction is modeled with static multipole expansion points located at atoms and bond centers. The polarization energy is modeled with anisotropic dipole polarizability tensors located at the centroids of localized bond and lone pair orbitals of the molecules. In the electric fields of the QM nuclei, electrons, and static multipoles of other EFPs, the polarizability tensors generate induced dipoles. The interactions between the induced dipoles in different molecules are also considered in the EFP method. The induced dipole moments (written as a column vector  $\boldsymbol{\mu}$ ) satisfy the following matrix equation:<sup>13</sup>

$$\mathbf{D}\boldsymbol{\mu} = \mathbf{F}, \quad (1)$$

where  $\mathbf{F}$  is a set of electrostatic fields at the polarizability points due to QM nuclei (nuc) and electrons (ele) and EFP static multipoles (mul) (the EFP induced dipole fields are not included),

$$\mathbf{F} = \mathbf{F}^{\text{nuc}} + \mathbf{F}^{\text{ele}} + \mathbf{F}^{\text{mul}}. \quad (2)$$

The elements of the matrix  $\mathbf{D}$  are a function of the polarizability tensors and the Cartesian coordinates of the polarizability points,

<sup>a)</sup>Author to whom correspondence should be addressed. Electronic mail: mark@si.fi.ameslab.gov

$$\mathbf{D}_{ii} = (\boldsymbol{\alpha}_i)^{-1} = \begin{pmatrix} \alpha_{i,xx} & \alpha_{i,xy} & \alpha_{i,xz} \\ \alpha_{i,yx} & \alpha_{i,yy} & \alpha_{i,yz} \\ \alpha_{i,zx} & \alpha_{i,zy} & \alpha_{i,zz} \end{pmatrix}^{-1}. \quad (3)$$

If  $i$  and  $j$  belong to the same molecule, the off-diagonal elements of  $\mathbf{D}$  are  $3 \times 3$  zero matrices,

$$\mathbf{D}_{ij} = \begin{pmatrix} 0 & 0 & 0 \\ 0 & 0 & 0 \\ 0 & 0 & 0 \end{pmatrix}. \quad (4)$$

Otherwise,

$$\mathbf{D}_{ij} = \begin{pmatrix} \frac{1}{r_{ij}^3} - \frac{3x_{ij}x_{ij}}{r_{ij}^5} & -\frac{3x_{ij}y_{ij}}{r_{ij}^5} & -\frac{3x_{ij}z_{ij}}{r_{ij}^5} \\ -\frac{3y_{ij}x_{ij}}{r_{ij}^5} & \frac{1}{r_{ij}^3} - \frac{3y_{ij}y_{ij}}{r_{ij}^5} & -\frac{3y_{ij}z_{ij}}{r_{ij}^5} \\ -\frac{3z_{ij}x_{ij}}{r_{ij}^5} & -\frac{3z_{ij}y_{ij}}{r_{ij}^5} & \frac{1}{r_{ij}^3} - \frac{3z_{ij}z_{ij}}{r_{ij}^5} \end{pmatrix}, \quad (5)$$

where  $\mathbf{r}_i = (x_i, y_i, z_i)$  and  $\mathbf{r}_j = (x_j, y_j, z_j)$  are the Cartesian coordinates of polarizability points  $i$  and  $j$ .

The induced dipoles can be obtained from the inverse of  $\mathbf{D}$ ,

$$\boldsymbol{\mu} = \mathbf{D}^{-1}\mathbf{F}. \quad (6)$$

However, iterative methods based on Eq. (7) are more common,

$$\boldsymbol{\mu}_i = \boldsymbol{\alpha}_i \left( \mathbf{F}_i - \sum_{j \neq i} \mathbf{D}_{ij} \boldsymbol{\mu}_j \right). \quad (7)$$

An initial guess (usually zero or from a previous calculation) of the induced dipoles can be substituted into the right side of Eq. (7) to produce a new set of induced dipoles on the left side of Eq. (7). In the EFP method, the simplest Jacobi single-point iterative method<sup>14</sup> is implemented. The convergence criterion is that the differences between the induced dipoles in two consecutive iterations are all smaller than  $10^{-10}$  a.u. Usually 10–13 iterations are required to reach convergence.

In QM/EFP calculations, the EFP interactions, which include the induced dipoles, are incorporated into the Hamiltonian to determine the electronic wave function and energy,

$$\mathbf{E} = \langle \Psi | (\mathbf{H}^0 + \mathbf{V}^{\text{EFP}}) | \Psi \rangle. \quad (8)$$

The polarization energy of the induced dipoles in the field is the reversible work required to charge the field  $\mathbf{F}$  from zero to full strength (both  $\boldsymbol{\mu}$  and  $\mathbf{F}$  are column vectors),<sup>3,8,15</sup>

$$\begin{aligned} G_{\text{pol}} &= - \int_0^{\text{full}} \boldsymbol{\mu}^T d\mathbf{F} = - \int_0^{\text{full}} (\mathbf{D}^{-1}\mathbf{F})^T d\mathbf{F} \\ &= - \int_0^{\text{full}} \mathbf{F}^T (\mathbf{D}^{-1})^T d\mathbf{F} \\ &= - \frac{1}{2} \mathbf{F}^T (\mathbf{D}^{-1})^T \mathbf{F} = - \frac{1}{2} \boldsymbol{\mu}^T \mathbf{F}. \end{aligned} \quad (9)$$

Note that the following expressions for  $G_{\text{pol}}$  are equivalent,

$$G_{\text{pol}} = - \frac{1}{2} \mathbf{F}^T (\mathbf{D}^{-1})^T \mathbf{F} = - \frac{1}{2} \boldsymbol{\mu}^T \mathbf{F} = - \frac{1}{2} \mathbf{F}^T \boldsymbol{\mu} = - \frac{1}{2} \mathbf{F}^T \mathbf{D}^{-1} \mathbf{F}. \quad (10)$$

The transpose of  $\mathbf{D}^{-1}$  in Eq. (10) does not affect the final value of  $G_{\text{pol}}$ .

Based on the last expression in Eq. (10), the derivative of the polarization energy  $G_{\text{pol}}$  with respect to a translational or rotational coordinate,  $s$ , is

$$\begin{aligned} \partial G_{\text{pol}} / \partial s &= - \frac{1}{2} (\partial \mathbf{F} / \partial s)^T \mathbf{D}^{-1} \mathbf{F} - \frac{1}{2} \mathbf{F}^T (\partial \mathbf{D}^{-1} / \partial s) \mathbf{F} \\ &\quad - \frac{1}{2} \mathbf{F}^T \mathbf{D}^{-1} (\partial \mathbf{F} / \partial s). \end{aligned} \quad (11)$$

Since  $\boldsymbol{\mu} = \mathbf{D}^{-1}\mathbf{F}$ , the first term in Eq. (11) can be written as

$$- \frac{1}{2} (\partial \mathbf{F} / \partial s)^T \mathbf{D}^{-1} \mathbf{F} = - \frac{1}{2} (\partial \mathbf{F} / \partial s)^T \boldsymbol{\mu}. \quad (12)$$

The third term in Eq. (11) can be written as

$$- \frac{1}{2} \mathbf{F}^T \mathbf{D}^{-1} (\partial \mathbf{F} / \partial s) = - \frac{1}{2} (\partial \mathbf{F} / \partial s)^T (\mathbf{D}^{-1})^T \mathbf{F}. \quad (13)$$

Defining

$$\tilde{\boldsymbol{\mu}} = (\mathbf{D}^{-1})^T \mathbf{F}, \quad (14)$$

Eq. (13) becomes

$$- \frac{1}{2} \mathbf{F}^T \mathbf{D}^{-1} (\partial \mathbf{F} / \partial s) = - \frac{1}{2} (\partial \mathbf{F} / \partial s)^T \tilde{\boldsymbol{\mu}}. \quad (15)$$

If the polarizability tensors are not symmetric,  $\tilde{\boldsymbol{\mu}}$  is different from  $\boldsymbol{\mu}$ . Combining the first and third terms in Eq. (11) leads to

$$\begin{aligned} & - \frac{1}{2} (\partial \mathbf{F} / \partial s)^T \mathbf{D}^{-1} \mathbf{F} - \frac{1}{2} \mathbf{F}^T \mathbf{D}^{-1} (\partial \mathbf{F} / \partial s) \\ &= - \frac{1}{2} (\partial \mathbf{F} / \partial s)^T \boldsymbol{\mu} - \frac{1}{2} (\partial \mathbf{F} / \partial s)^T \tilde{\boldsymbol{\mu}} \\ &= - (\partial \mathbf{F} / \partial s)^T \cdot \left( \frac{\boldsymbol{\mu} + \tilde{\boldsymbol{\mu}}}{2} \right). \end{aligned} \quad (16)$$

The second term of Eq. (11) contains the derivative of the inverse of  $\mathbf{D}$ , and is difficult to evaluate directly. Using the standard relation

$$\partial \mathbf{D}^{-1} / \partial s = - \mathbf{D}^{-1} (\partial \mathbf{D} / \partial s) \mathbf{D}^{-1}, \quad (17)$$

the derivative of the inverse of  $\mathbf{D}$  can be expressed as the much simpler derivative of  $\mathbf{D}$ . The inverse of  $\mathbf{D}$  can be combined with  $\mathbf{F}$  to form  $\boldsymbol{\mu}$  and  $\tilde{\boldsymbol{\mu}}$

$$\begin{aligned} & - \frac{1}{2} \mathbf{F}^T (\partial \mathbf{D}^{-1} / \partial s) \mathbf{F} \\ &= \frac{1}{2} \mathbf{F}^T \mathbf{D}^{-1} (\partial \mathbf{D} / \partial s) \mathbf{D}^{-1} \mathbf{F} \\ &= \frac{1}{2} (\tilde{\boldsymbol{\mu}})^T (\partial \mathbf{D} / \partial s) \boldsymbol{\mu}. \end{aligned} \quad (18)$$

So,

$$\begin{aligned} \partial G_{\text{pol}} / \partial s &= - (\partial \mathbf{F} / \partial s)^T \cdot \left( \frac{\boldsymbol{\mu} + \tilde{\boldsymbol{\mu}}}{2} \right) + \frac{1}{2} (\tilde{\boldsymbol{\mu}})^T (\partial \mathbf{D} / \partial s) \boldsymbol{\mu} \\ &= - \sum_i^N (\partial \mathbf{F}_i / \partial s) \left( \frac{\boldsymbol{\mu}_i + \tilde{\boldsymbol{\mu}}_i}{2} \right) \\ &\quad + \frac{1}{2} \sum_i^N \sum_j^N \tilde{\boldsymbol{\mu}}_i (\partial \mathbf{D}_{ij} / \partial s) \boldsymbol{\mu}_j \end{aligned} \quad (19)$$

where  $i$  and  $j$  run over all of the  $N$  induced dipoles. The first term in Eq. (19) contains the forces (or torques) on the in-

duced dipoles due to the electric fields of the QM atoms and the EFP static multipoles; the second term contains the forces (or torques) on the induced dipoles due to other induced dipoles.

As for  $\boldsymbol{\mu}$  [Eq. (7)],  $\tilde{\boldsymbol{\mu}}$  can also be determined iteratively using

$$\tilde{\boldsymbol{\mu}}_i = \boldsymbol{\alpha}_i^T \left( \mathbf{F}_i + \sum_{j \neq i} \mathbf{D}_{ij} \tilde{\boldsymbol{\mu}}_j \right). \quad (20)$$

As shown in Eq. (19), the derivatives of the electric fields,  $\partial \mathbf{F} / \partial s$ , which include the contributions from EFP static multipoles and QM nuclei and electrons at the polarizability points, are required to evaluate the polarization energy gradients. The derivatives of the electric fields due to EFP static multipoles and QM nuclei are straightforward. The derivatives of the QM electronic field are more complicated because the electronic wave function and density depend on the induced dipoles. Approximations have been employed to form the QM/EFP Fock operator in the self-consistent field (SCF) calculations and in the gradient evaluations, as described in Ref. 8. With these approximations, the derivatives of the electric field due to the QM electrons can be evaluated simply with the optimized electronic wave function and the derivatives of the basis functions.

In QM/EFP calculations the internal geometries of the molecules treated with the EFP method are frozen, and both the translational and rotational gradients (forces and torques) are required in geometry optimizations. A detailed analysis of the polarization forces and torques on the molecules treated with the EFP method can be found in Refs. 8 and 13. In EFP calculations without QM atoms, the exact gradients can be evaluated and molecular dynamics simulations can be performed.<sup>13</sup> When QM atoms are involved, approximate gradients are implemented and geometry optimizations and numerical Hessian analyses can be performed.<sup>8</sup> It is noted here that the errors in the gradients caused by various approximations (including the one that assumes  $\tilde{\boldsymbol{\mu}} = \boldsymbol{\mu}$ ) in the QM-EFP method are very small ( $< 10^{-6}$  a.u.) and do not cause noticeable problems in geometry optimizations and Hessian calculations.

## B. PCM

In a PCM calculation, the solute molecule is placed in a bulk solvent described as a polarizable continuum with a dielectric constant  $\epsilon$ . In this study only the conductorlike C-PCM, which in principle is applicable to conductors with  $\epsilon = \infty$ , is considered. However, it is common<sup>11,16,17</sup> to use C-PCM for solvents with  $\epsilon < \infty$  via simply scaling the apparent surface charges by a factor, selected to be  $(\epsilon - 1) / \epsilon$  in this study. Then, the energy and gradient expressions contain corresponding scaling factors. The cavity that the solute molecule occupies in the bulk solvent can be defined in a variety of ways. The most popular of these is to use interlocking spheres centered at atoms or atomic groups. The surface of the cavity is the boundary between the solute and solvent. In the PCM the ASC method is used to describe the electrostatic interaction between the solute and the bulk solvent. To

numerically solve the electrostatic boundary equation the continuous charge distribution on the boundary surface is divided into a set of point charges at a finite number of boundary surface elements, called tesserae. In the QM/PCM method, the solute is treated with QM methods, and the solute electrostatic potential is the sum of the potentials from the nuclei and electrons. The induced surface charges are used to form one-electron operators in the SCF calculation.

Based on the GEnErating-POLyhedra (GEPOL) (Refs. 17 and 18) cavity construction and surface tessellation procedure, the PCM ASCs, written as a vertical vector  $\mathbf{q}$ , are obtained by solving the matrix equation

$$\mathbf{C}\mathbf{q} = -\mathbf{V}, \quad (21)$$

where the vertical vector  $\mathbf{V}$  is the solute electrostatic potential and  $\mathbf{C}$  is the following matrix:

$$C_{ii} = 1.07 \frac{\epsilon}{\epsilon - 1} \sqrt{\frac{4\pi}{a_i}}, \quad (22)$$

$$C_{ij} = \frac{\epsilon}{\epsilon - 1} \cdot \frac{1}{|\mathbf{r}_i - \mathbf{r}_j|}. \quad (23)$$

The  $r_i$  and  $a_i$  are the coordinates and area, respectively, for tessera  $i$ , and  $\epsilon$  is the dielectric constant of the solvent.

To obtain  $\mathbf{q}$  from  $\mathbf{V}$  the inverse of  $\mathbf{C}$  can be used,

$$\mathbf{q} = -\mathbf{C}^{-1}\mathbf{V}. \quad (24)$$

Both direct matrix inversion and semi-iterative-interpolation techniques can be formulated to solve Eq. (24) for the PCM apparent surface charges.

In QM/PCM calculations, the potential of the PCM apparent surface charges is incorporated into the Hamiltonian to determine the electronic wavefunction and energy:

$$\mathbf{E} = \langle \Psi | (\mathbf{H}^0 + \mathbf{V}^{\text{PCM}}) | \Psi \rangle. \quad (25)$$

In each SCF step the PCM apparent surface charges are re-evaluated based on the current electron density and the electronic potential. Both the electron density and PCM surface charges are iterated to self-consistency when the SCF finishes.

As for the induced dipole polarization energy [Eqs. (9) and (10)], the total PCM polarization (or solvation) energy is<sup>6</sup>

$$G_{\text{sol}} = \frac{1}{2} \mathbf{q}^T \mathbf{V} = \frac{1}{2} \mathbf{V}^T \mathbf{q} = -\frac{1}{2} \mathbf{V}^T \mathbf{C}^{-1} \mathbf{V}. \quad (26)$$

The derivative of the PCM solvation energy  $G_{\text{sol}}$  with respect to a translational or rotational coordinate,  $s$ , of the solute is [Eqs. (17), (19), and (21) and note  $\mathbf{C}^{-1} = (\mathbf{C}^{-1})^T$ ],

$$\begin{aligned} \partial G_{\text{sol}} / \partial s &= -\frac{1}{2} (\partial \mathbf{V} / \partial s)^T \mathbf{C}^{-1} \mathbf{V} - \frac{1}{2} \mathbf{V}^T (\partial \mathbf{C}^{-1} / \partial s) \mathbf{V} \\ &\quad - \frac{1}{2} \mathbf{V}^T \mathbf{C}^{-1} (\partial \mathbf{V} / \partial s) \\ &= \sum_n^N (\partial V_n / \partial s) q_n + \frac{1}{2} \sum_n^N \sum_m^N q_n (\partial C_{nm} / \partial s) q_m, \quad (27) \end{aligned}$$

where  $m$  and  $n$  run over all of the  $N$  tesserae. The first term in Eq. (27) sums the forces (or torques) between the solute and the PCM surface charges; the second term sums the

forces (or torques) between the PCM surface charges themselves.

The derivatives of the total potentials  $\partial V/\partial s$  (i.e., fields) at the tesserae are required to evaluate the PCM solvation energy gradients. The fields due to QM nuclei are straightforward. The fields due to QM electrons can be evaluated simply with the optimized electronic wave function and the density. In principle, the analytic derivatives of the  $\mathbf{C}$  matrix elements ( $\partial C_{nm}/\partial s$ ) can be evaluated with the derivatives of the tessera positions and areas according to the GEPOL surface tessellation procedure [Eqs. (22) and (23)]. However, because the PCM potential energy surfaces are not continuous as a result of discrete tessellation, approximate and simplified derivatives of the  $\mathbf{C}$  matrix elements can be applied in the evaluation of Eq. (27). The details of the approximation and simplification can be found in Ref. 17. The approximate PCM solvation energy gradients are sufficient for molecular geometry optimization and Hessian analyses. A comparison between the gradients obtained by the approximate equations (analytic ones) and finite displacement (numerical ones) can be found in Ref. 17.

### C. QM/EFP/PCM and EFP/PCM

In a QM/EFP/PCM calculation, the electrostatic potentials at the tesserae due to QM atoms, EFP static multipoles (up to quadrupoles), and EFP induced dipoles are used to obtain the PCM induced surface charges [Eq. (24)],

$$\mathbf{q} = -\mathbf{C}^{-1}(\mathbf{V}^{\text{nuc}} + \mathbf{V}^{\text{ele}} + \mathbf{V}^{\text{mul}} + \mathbf{V}^{\mu}). \quad (28)$$

The EFP induced dipoles are determined by the electrostatic fields from the QM atoms, EFP multipoles, and PCM surface charges [Eq. (6)],

$$\boldsymbol{\mu} = \mathbf{D}^{-1}(\mathbf{F}^{\text{nuc}} + \mathbf{F}^{\text{ele}} + \mathbf{F}^{\text{mul}} + \mathbf{F}^q). \quad (29)$$

The electrostatic potentials generated by the PCM surface charges, the EFP static multipoles, and induced dipoles are added to the Hamiltonian to determine the electronic wave function and energy,

$$\mathbf{E} = \langle \Psi | (\mathbf{H}^0 + \mathbf{V}^{\text{EFP}} + \mathbf{V}^{\text{PCM}}) | \Psi \rangle. \quad (30)$$

The QM wave functions, EFP induced dipoles, and PCM ASCs are iterated to self-consistency as the SCF is converged.

To facilitate the analysis of the gradients of the EFP polarization energy and PCM solvation energy for the QM/EFP/PCM methods, the matrix equations [Eqs. (28) and (29)] are rearranged and combined to form a supermatrix equation, described in the following paragraphs.

Equation (29) can be written as

$$\mathbf{D}\boldsymbol{\mu} - \mathbf{F}^q = \mathbf{F}^{\text{nuc}} + \mathbf{F}^{\text{ele}} + \mathbf{F}^{\text{mul}}. \quad (31)$$

Based on Eq. (31), at the  $i$ th EFP induced dipole,

$$\sum_m \mathbf{D}_{im} \boldsymbol{\mu}_m - \sum_n \frac{-(\mathbf{r}_i - \mathbf{r}_n)}{|\mathbf{r}_i - \mathbf{r}_n|^3} q_n = \mathbf{F}_i = \mathbf{F}_i^{\text{nuc}} + \mathbf{F}_i^{\text{ele}} + \mathbf{F}_i^{\text{mul}}, \quad (32a)$$

$$\sum_m \mathbf{D}_{im} \boldsymbol{\mu}_m + \sum_n \mathbf{R}_{in} q_n = \mathbf{F}_i, \quad (32b)$$

where  $m$  runs over all of the EFP induced dipoles and  $n$  runs over all of the PCM induced charges,  $\mathbf{r}_i$  and  $\mathbf{r}_n$  are the Cartesian coordinates of the  $i$ th induced dipole and the  $n$ th induced charge, respectively,  $\mathbf{F}_i$  is the electrostatic field at the  $i$ th induced dipole due to the QM atoms and the EFP static multipoles. The second term on the left side of Eq. (32b) is the (negative) electrostatic field at the  $i$ th induced dipole due to all of the PCM induced charges. Note that both  $\boldsymbol{\mu}_m$  and  $q_n$  in Eq. (32b) are unknowns.

Similarly, Eq. (28) can be written as

$$\mathbf{V}^{\mu} + \mathbf{C}\mathbf{q} = -(\mathbf{V}^{\text{nuc}} + \mathbf{V}^{\text{ele}} + \mathbf{V}^{\text{mul}}). \quad (33)$$

Based on Eq. (33), at the  $j$ th tessera in the PCM calculation,

$$\sum_m \frac{-(\mathbf{r}_j - \mathbf{r}_m)}{|\mathbf{r}_j - \mathbf{r}_m|^3} \boldsymbol{\mu}_m + \sum_n \mathbf{C}_{jn} q_n = -\mathbf{V}_j = -(\mathbf{V}_j^{\text{nuc}} + \mathbf{V}_j^{\text{ele}} + \mathbf{V}_j^{\text{mul}}), \quad (34a)$$

$$\sum_m (\mathbf{R}^T)_{jm} \boldsymbol{\mu}_m + \sum_n \mathbf{C}_{jn} q_n = -\mathbf{V}_j, \quad (34b)$$

where  $m$  runs over all of the EFP induced dipoles and  $n$  runs over all of the PCM induced charges,  $\mathbf{r}_j$  and  $\mathbf{r}_m$  are the Cartesian coordinates of the  $j$ th induced charge and the  $m$ th induced dipole, respectively, and  $\mathbf{V}_j$  is the electrostatic potential at the  $j$ th induced charge due to the QM atoms and the EFP static multipoles. The first term on the left side of Eq. (34b) is the electrostatic potential at the  $j$ th induced charge due to all of the EFP induced dipoles. Again, note that both  $\boldsymbol{\mu}_m$  and  $q_n$  in Eq. (34b) are unknowns.

There are a total of  $m$  EFP induced dipoles and  $n$  PCM induced charges that satisfy Eqs. (32b) and (34b), respectively. Combining these  $m+n$  equations, a supermatrix equation is established,

$$\mathbf{B} \cdot \mathbf{w} = \mathbf{p}, \quad (35)$$

where  $\mathbf{p}$  is a combined set of the electrostatic fields at the polarizability points and the (negative) potentials at the PCM tesserae due to QM molecules and EFP static multipoles (note that the field due to PCM charges,  $\mathbf{F}^q$ , and the potential due to EFP induced dipoles,  $\mathbf{V}^{\mu}$ , are not included),  $\mathbf{w}$  is a combined set of induced dipoles and surface charges,

$$\mathbf{p} = \begin{pmatrix} \mathbf{F}_1 \\ \vdots \\ \mathbf{F}_m \\ -\mathbf{V}_1 \\ \vdots \\ -\mathbf{V}_n \end{pmatrix}, \quad (36)$$

$$\mathbf{w} = \begin{pmatrix} \boldsymbol{\mu}_1 \\ \vdots \\ \boldsymbol{\mu}_m \\ \mathbf{q}_1 \\ \vdots \\ \mathbf{q}_n \end{pmatrix}, \quad (37)$$

and  $\mathbf{B}$  is a geometric matrix, which can be written in block form as

$$\mathbf{B} = \begin{pmatrix} \mathbf{D} & \mathbf{R} \\ \mathbf{R}^T & \mathbf{C} \end{pmatrix}. \quad (38)$$

The  $\mathbf{D}$  and  $\mathbf{C}$  blocks are exactly the  $\mathbf{D}$  and  $\mathbf{C}$  matrices in Eqs. (1) and (21), with dimensions  $m \times m$  and  $n \times n$ , respectively. The elements of the  $m \times n$  matrix  $\mathbf{R}$  are operators [Eq. (32)] that act on the  $n$ th induced PCM surface charge to produce (negative) electrostatic fields at the  $m$ th EFP polarizability point,

$$R_{mn} = \frac{\mathbf{r}_m - \mathbf{r}_n}{|\mathbf{r}_m - \mathbf{r}_n|^3}, \quad (39)$$

where  $\mathbf{r}_n$  and  $\mathbf{r}_m$  are the Cartesian coordinates of the induced charge  $n$  and the induced dipole  $m$ , respectively.

$\mathbf{R}^T$  is the transpose of  $\mathbf{R}$ , with a dimension of  $n \times m$ . The elements of  $\mathbf{R}^T$  are operators [Eq. (34)] that act on the  $m$ th induced dipoles to produce electrostatic potentials at the  $n$ th PCM tesserae,

$$(R^T)_{nm} = -\frac{\mathbf{r}_n - \mathbf{r}_m}{|\mathbf{r}_n - \mathbf{r}_m|^3} = \frac{\mathbf{r}_m - \mathbf{r}_n}{|\mathbf{r}_m - \mathbf{r}_n|^3} = R_{mn}. \quad (40)$$

The physical meaning of the supermatrix [Eq. (35)] is that the EFP induced dipoles and PCM induced charges are uniquely determined by the field and potential of the QM nuclei and electrons, and the EFP static multipoles; therefore, the right side of Eq. (35) involves only the field/potential due to QM atoms and EFP static multipoles, and the left side involves only the induced EFP dipoles and PCM charges. The interaction between the induced dipoles and charges is implicitly described with the matrices  $\mathbf{R}$  and  $\mathbf{R}^T$ , just as the interaction between the EFP induced dipoles is implicitly described with the off-diagonal elements of matrix  $\mathbf{D}$ , and the interaction between the PCM induced charges is implicitly described with the off-diagonal elements of matrix  $\mathbf{C}$ .

The supermatrix equation [Eq. (35)] can be solved iteratively using Eqs. (28) and (29), as implemented here and in previous studies.<sup>12</sup>

As for the EFP polarization energy [Eqs. (9) and (10)] and the PCM solvation energy [Eq. (26)], the combined EFP-PCM polarization energy is

$$\begin{aligned} G_{\text{pol+sol}} &= -\frac{1}{2} \mathbf{p}^T \mathbf{w} = -\frac{1}{2} \mathbf{p}^T \mathbf{B}^{-1} \mathbf{p} \\ &= -\frac{1}{2} \boldsymbol{\mu}^T (\mathbf{F}^{\text{nuc}} + \mathbf{F}^{\text{ele}} + \mathbf{F}^{\text{mul}}) \\ &\quad + \frac{1}{2} \mathbf{q}^T (\mathbf{V}^{\text{nuc}} + \mathbf{V}^{\text{ele}} + \mathbf{V}^{\text{mul}}). \end{aligned} \quad (41)$$

The derivative of the energy  $G_{\text{pol+sol}}$  with respect to a translational or rotational coordinate,  $s$ , is thus [Eqs. (19) and (27)],

$$\begin{aligned} \partial G_{\text{pol+sol}} / \partial s &= -\frac{1}{2} (\partial \mathbf{p} / \partial s)^T \mathbf{B}^{-1} \mathbf{p} - \frac{1}{2} \mathbf{p}^T (\partial \mathbf{B}^{-1} / \partial s) \mathbf{p} \\ &\quad - \frac{1}{2} \mathbf{p}^T \mathbf{B}^{-1} (\partial \mathbf{p} / \partial s) \end{aligned} \quad (42a)$$

$$= -\frac{1}{2} (\partial \mathbf{p} / \partial s)^T (\tilde{\mathbf{w}} + \mathbf{w}) + \frac{1}{2} \tilde{\mathbf{w}}^T (\partial \mathbf{B} / \partial s) \mathbf{w}, \quad (42b)$$

where  $\tilde{\mathbf{w}}$  is defined as

$$\tilde{\mathbf{w}} = (\mathbf{B}^{-1})^T \mathbf{p}, \quad (43)$$

or separately [Eqs. (28) and (29)],

$$\tilde{\mathbf{q}} = -(\mathbf{C}^{-1})^T (\mathbf{V}^{\text{nuc}} + \mathbf{V}^{\text{ele}} + \mathbf{V}^{\text{mul}} + \mathbf{V}^{\tilde{\boldsymbol{\mu}}}), \quad (44)$$

$$\tilde{\boldsymbol{\mu}} = (\mathbf{D}^{-1})^T (\mathbf{F}^{\text{nuc}} + \mathbf{F}^{\text{ele}} + \mathbf{F}^{\text{mul}} + \mathbf{F}^{\tilde{\mathbf{q}}}). \quad (45)$$

Since various approximations have been introduced in the evaluations of the derivatives of the QM fields<sup>8</sup> and the derivatives of the  $\mathbf{C}$  matrix elements,<sup>17</sup> both the EFP polarization energy gradient and the PCM solvation energy gradient are approximate. To simplify the computer program development for the solution of two sets of PCM induced charges [Eqs. (28) and (44)], in this study  $\tilde{\mathbf{q}}$  in Eq. (44) is not actually evaluated but approximated with  $\mathbf{q}$ ,

$$\begin{aligned} \tilde{\mathbf{q}} &= -(\mathbf{C}^{-1})^T (\mathbf{V}^{\text{nuc}} + \mathbf{V}^{\text{ele}} + \mathbf{V}^{\text{mul}} + \mathbf{V}^{\tilde{\boldsymbol{\mu}}}) \\ &\approx -\mathbf{C}^{-1} (\mathbf{V}^{\text{nuc}} + \mathbf{V}^{\text{ele}} + \mathbf{V}^{\text{mul}} + \mathbf{V}^{\boldsymbol{\mu}}) = \mathbf{q}, \end{aligned} \quad (46)$$

and  $\tilde{\boldsymbol{\mu}}$  in Eq. (45) is evaluated approximately with  $\mathbf{q}$  instead of  $\tilde{\mathbf{q}}$ ,

$$\begin{aligned} \tilde{\boldsymbol{\mu}} &= (\mathbf{D}^{-1})^T (\mathbf{F}^{\text{nuc}} + \mathbf{F}^{\text{ele}} + \mathbf{F}^{\text{mul}} + \mathbf{F}^{\tilde{\mathbf{q}}}) \\ &\approx (\mathbf{D}^{-1})^T (\mathbf{F}^{\text{nuc}} + \mathbf{F}^{\text{ele}} + \mathbf{F}^{\text{mul}} + \mathbf{F}^{\mathbf{q}}). \end{aligned} \quad (47)$$

$\tilde{\boldsymbol{\mu}}$  is different from  $\boldsymbol{\mu}$  since in the EFP method  $(\mathbf{D}^{-1})^T \neq \mathbf{D}^{-1}$  due to the asymmetry of the polarizability tensors. It is emphasized that the errors of the approximations in Eqs. (46) and (47) are considerably smaller than those introduced in the approximate derivatives of the  $\mathbf{C}$  matrix elements,<sup>17</sup> as assessed by comparing the numerical gradients obtained from small displacements to the analytic gradients obtained with the approximate equations for both EFP/PCM calculations with and without induced dipoles. There is little benefit to use the rigorous equations [Eqs. (44) and (45)] because of the current approximations in the PCM gradients. Similar approximation (i.e., using only one set of charges) has been successfully used in the calculation of the solvation energy gradients in the PCM (IEF-PCM) method in which the  $\mathbf{C}$  matrix is not symmetric, and two sets of charges appear in the rigorous gradient expression.<sup>17,19</sup>

The first term in Eq. (42b) contains the forces (or torques) between (1) QM nuclei and induced dipoles, (2) QM nuclei and PCM surface charges, (3) QM electrons and induced dipoles, (4) QM electrons and PCM surface charges, (5) EFP static multiples and induced dipoles, and (6) EFP static multiples and PCM surface charges,

$$\begin{aligned}
& -\frac{1}{2}(\partial\mathbf{p}/\partial s)^T(\tilde{\mathbf{w}} + \mathbf{w}) \\
& = -\frac{1}{2}(\partial\mathbf{F}/\partial s)^T(\tilde{\boldsymbol{\mu}} + \boldsymbol{\mu}) + \frac{1}{2}(\partial\mathbf{V}/\partial s)^T(\tilde{\mathbf{q}} + \mathbf{q}) \\
& \approx -\frac{1}{2}(\partial\mathbf{F}^{\text{nuc}}/\partial s)^T(\tilde{\boldsymbol{\mu}} + \boldsymbol{\mu}) - \frac{1}{2}(\partial\mathbf{F}^{\text{ele}}/\partial s)^T(\tilde{\boldsymbol{\mu}} + \boldsymbol{\mu}) \\
& \quad - \frac{1}{2}(\partial\mathbf{F}^{\text{mul}}/\partial s)^T(\tilde{\boldsymbol{\mu}} + \boldsymbol{\mu}) + (\partial\mathbf{V}^{\text{nuc}}/\partial s)^T\mathbf{q} \\
& \quad + (\partial\mathbf{V}^{\text{ele}}/\partial s)^T\mathbf{q} + (\partial\mathbf{V}^{\text{mul}}/\partial s)^T\mathbf{q} \\
& = -f_{\text{nuc-}\mu} - f_{\text{ele-}\mu} - f_{\text{mul-}\mu} - f_{\text{nuc-}q} - f_{\text{ele-}q} - f_{\text{mul-}q}. \quad (48)
\end{aligned}$$

Note that the final equality in Eq. (48) is an approximation because  $\tilde{\mathbf{q}} + \mathbf{q} \approx 2\mathbf{q}$  [Eqs. (46) and (47)] is used.

The second term of Eq. (42b) contains the forces (or torques) between (1) induced dipoles and induced dipoles, (2) induced dipoles and PCM surface charges, and (3) PCM surface charges and PCM surface charges (note that  $\mathbf{B}$  has four blocks,  $\mathbf{D}$ ,  $\mathbf{R}$ ,  $\mathbf{R}^T$  and  $\mathbf{C}$ , and  $(\mathbf{R}^T)^T = \mathbf{R}$ ),

$$\begin{aligned}
\frac{1}{2}\tilde{\mathbf{w}}^T(\partial\mathbf{B}/\partial s)\mathbf{w} & = \frac{1}{2}\tilde{\boldsymbol{\mu}}^T(\partial\mathbf{D}/\partial s)\boldsymbol{\mu} + \frac{1}{2}\tilde{\boldsymbol{\mu}}^T(\partial\mathbf{R}/\partial s)\mathbf{q} \\
& \quad + \frac{1}{2}\tilde{\mathbf{q}}^T(\partial\mathbf{R}^T/\partial s)\boldsymbol{\mu} + \frac{1}{2}\tilde{\mathbf{q}}^T(\partial\mathbf{C}/\partial s)\mathbf{q} \\
& = \frac{1}{2}\tilde{\boldsymbol{\mu}}^T(\partial\mathbf{D}/\partial s)\boldsymbol{\mu} + \frac{1}{2}\tilde{\boldsymbol{\mu}}^T(\partial\mathbf{R}/\partial s)\mathbf{q} \\
& \quad + \frac{1}{2}\boldsymbol{\mu}^T(\partial\mathbf{R}/\partial s)\tilde{\mathbf{q}} + \frac{1}{2}\tilde{\mathbf{q}}^T(\partial\mathbf{C}/\partial s)\mathbf{q} \\
& \approx \frac{1}{2}\tilde{\boldsymbol{\mu}}^T(\partial\mathbf{D}/\partial s)\boldsymbol{\mu} + \frac{1}{2}(\boldsymbol{\mu} + \tilde{\boldsymbol{\mu}})^T(\partial\mathbf{R}/\partial s)\mathbf{q} \\
& \quad + \frac{1}{2}\mathbf{q}^T(\partial\mathbf{C}/\partial s)\mathbf{q} = -f_{\mu-\mu} - f_{\mu-q} - f_{q-q}. \quad (49)
\end{aligned}$$

As for Eq. (48), the final equality in Eq. (49) is also an approximation.

The forces (or torques) between the QM nuclei and electrons, EFP static multipoles and the induced dipoles, as well as those between the induced dipoles themselves (i.e.,  $f_{\text{nuc-}\mu}$ ,  $f_{\text{ele-}\mu}$ ,  $f_{\text{mul-}\mu}$ , and  $f_{\mu-\mu}$ ) can be evaluated with the methods described in Sec. II A. The PCM-related forces, i.e., the forces (or torques) between the QM nuclei and electrons, EFP static multipoles, EFP induced dipoles, and the PCM surface charges, as well as those between the surface charges themselves (i.e.,  $f_{\text{nuc-}q}$ ,  $f_{\text{ele-}q}$ ,  $f_{\text{mul-}q}$ ,  $f_{\mu-q}$ , and  $f_{q-q}$ ) are more complicated because of the motions of the PCM tesserae. The forces  $f_{\text{nuc-}q}$ ,  $f_{\text{ele-}q}$ , and  $f_{q-q}$  have been discussed in Sec. II B. The forces and torques on EFPs by PCM surface charges are discussed next.

The force (or torque) between the EFP induced dipoles and the PCM surface charges can be rewritten in a form that is similar to that between the EFP static multipoles and the surface charges because the force can be evaluated either with the EFP induced dipoles and the gradient of the field of PCM charges, or with the PCM charges and the field of EFP induced dipoles,

$$\begin{aligned}
-f_{\mu-q} & = \frac{1}{2}(\boldsymbol{\mu} + \tilde{\boldsymbol{\mu}})^T(\partial\mathbf{R}/\partial s)\mathbf{q} \\
& = \frac{1}{2}(\partial\mathbf{V}^{\mu}/\partial s)^T\mathbf{q} + \frac{1}{2}(\partial\mathbf{V}^{\tilde{\mu}}/\partial s)^T\mathbf{q}. \quad (50)
\end{aligned}$$

Therefore the PCM related forces (or torques) can be expressed as

$$\begin{aligned}
-f_{\text{PCM}} & = -f_{\text{nuc-}q} - f_{\text{ele-}q} - f_{\text{mul-}q} - f_{\mu-q} - f_{q-q} \\
& = (\partial\mathbf{V}^{\text{nuc}}/\partial s)^T\mathbf{q} + (\partial\mathbf{V}^{\text{ele}}/\partial s)^T\mathbf{q} + (\partial\mathbf{V}^{\text{mul}}/\partial s)^T\mathbf{q} \\
& \quad + \left[ \frac{1}{2}(\partial\mathbf{V}^{\mu}/\partial s)^T\mathbf{q} + \frac{1}{2}(\partial\mathbf{V}^{\tilde{\mu}}/\partial s)^T\mathbf{q} \right] + \frac{1}{2}\mathbf{q}^T(\partial\mathbf{C}/\partial s)\mathbf{q} \\
& = (\partial\mathbf{V}^{\text{all}}/\partial s)^T\mathbf{q} + \frac{1}{2}\mathbf{q}^T(\partial\mathbf{C}/\partial s)\mathbf{q} \\
& = \sum_n^N (\partial V_n^{\text{all}}/\partial s)q_n + \frac{1}{2}\sum_n^N \sum_m^N q_n(\partial C_{nm}/\partial s)q_m, \quad (51)
\end{aligned}$$

where  $m$  and  $n$  run over all of the  $N$  tesserae, and

$$\mathbf{V}^{\text{all}} = \mathbf{V}^{\text{nuc}} + \mathbf{V}^{\text{ele}} + \mathbf{V}^{\text{mul}} + \frac{1}{2}\mathbf{V}^{\mu} + \frac{1}{2}\mathbf{V}^{\tilde{\mu}}. \quad (52)$$

Equation (51) is very similar to Eq. (27). The first term contains the electrostatic forces on the PCM surface charges due to the electric fields of the solute (including QM molecules, EFP static multipoles, and EFP induced dipoles). The second term contains the forces at the PCM surface charges by other surface charges.

In the following a detailed analysis is presented for the translational and rotational gradients with relevance to the PCM surface charges. To facilitate the analysis, the surface tesserae are divided into groups I and J. The group I tesserae are on the spheres associated with  $A$  (a QM atom or EFP); the group J tesserae are on the other spheres of the remaining atoms and EFPs, denoted collectively as  $B$ .

## D. Translational gradients

The PCM related translational gradient of a QM atom or an EFP, denoted as  $A$ , in the  $x$  direction is the derivative of the PCM solvation energy [Eqs. (27) and (51)] with respect to the Cartesian coordinate  $x_A$  of the atom or the EFP, as well as the Cartesian coordinates  $x_i$  of the group I tesserae, which are associated with  $A$ .

The motions of the tesserae corresponding to the translation of  $A$  are determined by the solute cavity construction and the surface tessellation schemes. Using the GEPOL-Gauss-Bonnet (GEPOL-GB),<sup>18</sup> GEPOL-Area Scaling (GEPOL-AS),<sup>17</sup> and GEPOL-Regular Tessellation (GEPOL-RT) (Ref. 17) schemes, the spheres are always centered at the EFP atomic centers (nuclei). In a given multigeometry calculation, the radii of the spheres are not subject to change when the geometry of the system changes. Therefore, when  $A$  (and only  $A$ ) translates by  $\partial x$ , the spheres associated with  $A$  translate exactly by  $\partial x$ , while the spheres associated with other atoms and EFPs do not move. Thus, the group I tesserae will translate exactly by  $\partial x$  with  $A$ , while the group J tesserae will not move; i.e.,  $\partial x_j = 0$  for  $j \in J$ . So, the displacement operator can be written as

$$\partial x = \partial x_A + \sum_i^I \partial x_i. \quad (53)$$

The differentiation operator is thus

$$\partial/\partial x = \partial/\partial x_A + \sum_i^I (\partial/\partial x_i), \quad (54)$$

where  $i$  runs over the group I tesserae.

$$\begin{aligned}
-f_{\text{PCM}} = & \sum_n^N (\partial V_n^{\text{all}}/\partial x_A) q_n + \frac{1}{2} \sum_n^N \sum_m^N q_n q_m (\partial C_{nm}/\partial x_A) \\
& + \sum_i^I (\partial V_i^{\text{all}}/\partial x_i) q_i + \frac{1}{2} \sum_i^I \sum_m^N q_i q_m (\partial C_{im}/\partial x_i) \\
& + \frac{1}{2} \sum_n^N \sum_i^I q_n q_i (\partial C_{ni}/\partial x_i). \quad (55)
\end{aligned}$$

Apparently, the second term in Eq. (55) is zero because the change of  $x_A$  has no effect on the coordinates of the tesserae, and the fourth and fifth terms can be combined because  $\mathbf{C}$  is symmetric. So,

$$\begin{aligned}
-f_{\text{PCM}} = & \sum_n^N (\partial V_n^{\text{all}}/\partial x_A) q_n + \sum_i^I (\partial V_i^{\text{all}}/\partial x_i) q_i \\
& + \sum_i^I \sum_m^N q_i q_m (\partial C_{im}/\partial x_i). \quad (56)
\end{aligned}$$

Furthermore, the third term in Eq. (56) can be simplified using the variable-tessera-number (VTN) approximation<sup>17</sup> in which the  $\mathbf{C}$  elements for the group I tesserae are constants and have zero derivatives (i.e.,  $\partial C_{ik}/\partial x_i = 0$  if  $i \in I$  and  $k \in I$ ),

$$\begin{aligned}
& \sum_i^I \sum_m^N q_i q_m (\partial C_{im}/\partial x_i) \\
= & \sum_i^I \sum_k^I q_i q_k (\partial C_{ik}/\partial x_i) + \sum_i^I \sum_j^J q_i q_j (\partial C_{ij}/\partial x_i) \\
= & \sum_i^I \sum_j^J q_i q_j (\partial C_{ij}/\partial x_i) \\
= & \sum_i^I \sum_j^J q_i q_j \left[ \partial \left( \frac{\epsilon}{\epsilon-1} \cdot \frac{1}{|\mathbf{r}_i - \mathbf{r}_j|} \right) / \partial x_i \right] \\
= & -\frac{\epsilon}{\epsilon-1} \sum_i^I \sum_j^J q_i q_j \frac{x_i - x_j}{|\mathbf{r}_i - \mathbf{r}_j|^3}. \quad (57)
\end{aligned}$$

Expanding the first term of Eq. (56) into group I and J tesserae,

$$\begin{aligned}
-f_{\text{PCM}} = & \sum_i^I (\partial V_i^{\text{all}}/\partial x_A) q_i + \sum_j^J (\partial V_j^{\text{all}}/\partial x_A) q_j \\
& + \sum_i^I (\partial V_i^{\text{all}}/\partial x_i) q_i - \frac{\epsilon}{\epsilon-1} \sum_i^I \sum_j^J q_i q_j \frac{x_i - x_j}{|\mathbf{r}_i - \mathbf{r}_j|^3}. \quad (58)
\end{aligned}$$

The total potential at a tessera can be separated into two terms, one due to A, the other due to B (the remaining QM atoms or EFPs),

$$V_n^{\text{all}} = V_n^A + V_n^B. \quad (59)$$

Only the potential due to A will change when A (and only A) is displaced. The first three terms in Eq. (58) can thus be expanded and then simplified (note  $\partial V_i^B/\partial x_A = 0$  and  $\partial V_j^B/\partial x_A = 0$ ):

$$\begin{aligned}
& \sum_i^I (\partial V_i^{\text{all}}/\partial x_A) q_i + \sum_j^J (\partial V_j^{\text{all}}/\partial x_A) q_j + \sum_i^I (\partial V_i^{\text{all}}/\partial x_i) q_i \\
= & \sum_i^I (\partial V_i^A/\partial x_A) q_i + \sum_i^I (\partial V_i^B/\partial x_A) q_i + \sum_j^J (\partial V_j^A/\partial x_A) q_j \\
& + \sum_j^J (\partial V_j^B/\partial x_A) q_j + \sum_i^I (\partial V_i^A/\partial x_i) q_i + \sum_i^I (\partial V_i^B/\partial x_i) q_i \\
= & \sum_i^I (\partial V_i^A/\partial x_A + \partial V_i^A/\partial x_i) q_i + \sum_j^J (\partial V_j^A/\partial x_A) q_j \\
& + \sum_i^I (\partial V_i^B/\partial x_i) q_i. \quad (60)
\end{aligned}$$

Since  $V_i^A$  depends only on the *relative* positions of  $x_A$  and  $x_i$ , simultaneous identical changes in both  $x_A$  and  $x_i$  result in zero change of  $V_i^A$ ,

$$\partial V_i^A/\partial x_A + \partial V_i^A/\partial x_i = 0. \quad (61)$$

So,

$$\begin{aligned}
-f_{\text{PCM}} = & \sum_i^I (\partial V_i/\partial x_A) q_i + \sum_j^J (\partial V_j/\partial x_A) q_j + \sum_i^I (\partial V_i/\partial x_i) q_i \\
& - \frac{\epsilon}{\epsilon-1} \sum_i^I \sum_j^J q_i q_j \frac{x_i - x_j}{|\mathbf{r}_i - \mathbf{r}_j|^3} \\
= & \sum_i^I (\partial V_i^B/\partial x_i) q_i + \sum_j^J (\partial V_j^A/\partial x_A) q_j \\
& - \frac{\epsilon}{\epsilon-1} \sum_i^I \sum_j^J q_i q_j \frac{x_i - x_j}{|\mathbf{r}_i - \mathbf{r}_j|^3} \\
= & \sum_i^I E_i^{B,x} q_i + \sum_j^J E_j^{A,x} q_j \\
& - \frac{\epsilon}{\epsilon-1} \sum_i^I \sum_j^J q_i q_j \frac{x_i - x_j}{|\mathbf{r}_i - \mathbf{r}_j|^3}, \quad (62)
\end{aligned}$$

where  $E_i^{B,x}$  and  $E_j^{A,x}$  are the electrostatic fields (in the  $x$  direction) at group I tesserae due to B and at group J tesserae due to A, respectively. Thus, the PCM related force has three terms: (1) the force on the group I ASCs (of A) by B, (2) the force on A by the ASCs on the group J spheres associated with B, and (3) the force on the group I ASCs by the group J ASCs.

## E. Rotational gradients

The PCM related rotational gradients of an EFP A about its center of mass (COM) in the  $x$  direction is the derivative of the PCM solvation energy [Eqs. (27) and (51)] with respect to the  $y$ - $z$  rotation plane of A, as well as the corresponding motions of the group I tesserae associated with A.

The overall rotation of A by a small angle  $\partial\theta$  in the  $y$ - $z$  plane about its center of mass can be decomposed into individual rotations of the EFP static point multipoles and induced dipoles in the  $y$ - $z$  plane (denoted as  $\theta_i^A$ ) about their

center points ( $x_a$ ,  $y_a$ , and  $z_a$ ) plus individual translations of the multipoles and induced dipoles in the  $y$ - $z$  plane,

$$\begin{aligned}\partial\theta_a^x &= \partial\theta, \\ \partial x_a &= 0, \\ \partial y_a &= -\partial\theta \cdot (z_a - z_{\text{COM}}^A), \\ \partial z_a &= \partial\theta \cdot (y_a - y_{\text{COM}}^A),\end{aligned}\quad (63)$$

where  $(x_{\text{COM}}^A, y_{\text{COM}}^A, z_{\text{COM}}^A)$  are the coordinates of the center of mass of  $A$ .

Using the GEPOL-GB, GEPOL-AS, and GEPOL-RT cavity construction and tessellation schemes, the spheres are always centered at EFP atomic centers (nuclei), so the sphere centers move (only translation, no rotation) when  $A$  rotates. The positions of the tesserae on a sphere relative to the sphere center are fixed, so the tesserae move (only translation) with the sphere centers. When  $A$  rotates by  $\partial\theta$  in the  $y$ - $z$  plane, the group I tesserae move by (note that there is no rotation)

$$\begin{aligned}\partial x_i &= 0, \\ \partial y_i &= -\partial\theta \cdot (z_{ic} - z_{\text{COM}}^A), \\ \partial z_i &= \partial\theta \cdot (y_{isc} - y_{\text{COM}}^A),\end{aligned}\quad (64)$$

where  $(x_{isc}, y_{isc}, z_{isc})$  is the center of the sphere on which the  $i$ th tessera is located.

However, the net torque of the molecular system is not zero if the individual torque of each fragment is derived using Eq. (64) and the VTN approximation because the individual torques are calculated with the forces on the sphere center points ( $x_{isc}, y_{isc}, z_{isc}$ ), while the total torque is calculated (or defined) with the forces on the tesserae, and the differences cannot be canceled if the VTN approximation is used. In geometry optimizations it is important and preferable that both the net forces and torques of the system are zero. Therefore, in the following, an alternative to Eq. (64) is discussed.

As discussed above, the positions of the tesserae on a sphere relative to the center of the sphere are fixed, so the tesserae move together with the sphere centers (no *relative* rotations). The rotations of the tesserae relative to the center of the sphere will, in principle (when an infinite number of tesserae are used), have no effect on the PCM solvation energy. In other words, the PCM solvation energy for a system is independent of the rotation or orientation of the molecule when an infinite number of tesserae are used. When a relatively small number of tesserae are used, the PCM solvation energy does change when the system rotates because of the discrete tessellation of the molecular surface. Using the GEPOL-AS tessellation scheme and 60 initial tesserae per sphere, the rotational variation of the PCM solvation energy is  $\sim 10^{-5}$  a.u. a relatively small value. So, assuming that the tesserae can rotate with the molecule will apparently not introduce significant errors in either the PCM solvation energy or the energy gradients.

Now, therefore, assume the tesserae can rotate with the molecule. When  $A$  rotates by a small angle  $\partial\theta$  in the  $y$ - $z$  plane, the group I tesserae move by [Eq. (64)],

$$\begin{aligned}\partial x_i &= 0, \\ \partial y_i &= -\partial\theta \cdot (z_i - z_{\text{COM}}^A), \\ \partial z_i &= \partial\theta \cdot (y_i - y_{\text{COM}}^A),\end{aligned}\quad (65)$$

where  $(x_i, y_i, z_i)$  are the coordinates of tessera  $i$ . So, the differentiation operator  $\partial/\partial\theta^x$  corresponding to the rotation of  $A$  (and the group I tesserae associated with  $A$ ) in the  $y$ - $z$  plane is the sum of Eqs. (63) and (65),

$$\begin{aligned}\partial/\partial\theta^x &= \sum_a^A [\partial/\partial\theta_a^x + (\partial/\partial z_a)(y_a - y_{\text{COM}}^A) \\ &\quad - (\partial/\partial y_a)(z_a - z_{\text{COM}}^A)] + \sum_i^I [(\partial/\partial z_i)(y_i - y_{\text{COM}}^A) \\ &\quad - (\partial/\partial y_i)(z_i - z_{\text{COM}}^A)].\end{aligned}\quad (66)$$

Therefore, the PCM related torque is [Eqs. (51), (56), and (57)],

$$\begin{aligned}-\tau_{\text{PCM}} &= \sum_n^N q_n \sum_a^A (\partial V_n^{\text{all}}/\partial\theta_a^x) + \sum_n^N q_n \sum_a^A [(\partial V_n^{\text{all}}/\partial z_a) \\ &\quad \times (y_a - y_{\text{COM}}^A) - (\partial V_n^{\text{all}}/\partial y_a)(z_a - z_{\text{COM}}^A)] \\ &\quad + \sum_i^I q_i [(\partial V_i^{\text{all}}/\partial z_i)(y_i - y_{\text{COM}}^A) \\ &\quad - (\partial V_i^{\text{all}}/\partial y_i)(z_i - z_{\text{COM}}^A)] \\ &\quad - \frac{\epsilon}{\epsilon - 1} \sum_i^I \sum_j^J q_i q_j \left[ \frac{z_i - z_j}{|\mathbf{r}_i - \mathbf{r}_j|^3} (y_i - y_{\text{COM}}^A) \right. \\ &\quad \left. - \frac{y_i - y_j}{|\mathbf{r}_i - \mathbf{r}_j|^3} (z_i - z_{\text{COM}}^A) \right].\end{aligned}\quad (67)$$

$V_n^{\text{all}}$  is the total potential (due to the QM atoms, EFP static multipoles, and EFP induced dipoles) at tessera  $n$ . However, only the potential due to the EFP static multipole or induced dipole point  $a$  will change when  $a$  (and only  $a$ ) rotates or translates,

$$\begin{aligned}\partial V_n^{\text{all}}/\partial\theta_a^x &= \partial V_n^a/\partial\theta_a^x, \\ \partial V_n^{\text{all}}/\partial z_a &= \partial V_n^a/\partial z_a = E_n^{a,z}, \\ \partial V_n^{\text{all}}/\partial y_a &= \partial V_n^a/\partial y_a = E_n^{a,y},\end{aligned}\quad (68)$$

where  $V_n^a$  is the potential at tessera  $n$  due to the EFP static multipole or induced dipole  $a$ .  $E_n^{a,z}$  and  $E_n^{a,y}$  are the fields at tessera  $n$  in the  $z$  and  $y$  directions, respectively, due to  $a$ .

$V_i^{\text{all}}$  is the total potential (due to the QM atoms, EFP static multipoles, and EFP induced dipoles) at tessera  $i$ . When  $A$  and the group I tesserae move, only the potential due to  $B$  will change, and the corresponding derivatives are the fields

$$\begin{aligned} \partial V_i^{\text{all}}/\partial z_i &= \partial V_i^A/\partial z_i + \partial V_i^B/\partial z_i = \partial V_i^B/\partial z_i = E_i^{B,z}, \\ \partial V_i^{\text{all}}/\partial y_i &= \partial V_i^A/\partial y_i + \partial V_i^B/\partial y_i = \partial V_i^B/\partial y_i = E_i^{B,y}. \end{aligned} \quad (69)$$

Using Eqs. (68) and (69), Eq. (67) becomes

$$\begin{aligned} -\tau_{\text{PCM}} &= \sum_n^N q_n \sum_a^A (\partial V_n^a/\partial \theta_a^x) + \sum_n^N q_n \sum_a^A [E_n^{a,z}(y_a - y_{\text{COM}}^A) \\ &\quad - E_n^{a,y}(z_a - z_{\text{COM}}^A)] + \sum_i^I q_i [E_i^{B,z}(y_i - y_{\text{COM}}^A) \\ &\quad - E_i^{B,y}(z_i - z_{\text{COM}}^A)] - \frac{\epsilon}{\epsilon - 1} \\ &\quad \times \sum_i^I \sum_j^J q_i q_j \left[ \frac{z_i - z_j}{|\mathbf{r}_i - \mathbf{r}_j|^3} (y_i - y_{\text{COM}}^A) \right. \\ &\quad \left. - \frac{y_i - y_j}{|\mathbf{r}_i - \mathbf{r}_j|^3} (z_i - z_{\text{COM}}^A) \right]. \end{aligned} \quad (70)$$

The first and second terms of the right side of Eq. (70) can be separated for groups I and J tesserae,

$$\begin{aligned} &\sum_i^I q_i \sum_a^A (\partial V_i^a/\partial \theta_a^x) + \sum_j^J q_j \sum_a^A (\partial V_j^a/\partial \theta_a^x) \\ &\quad + \sum_i^I q_i \sum_a^A [E_i^{a,z}(y_a - y_{\text{COM}}^A) - E_i^{a,y}(z_a - z_{\text{COM}}^A)] \\ &\quad + \sum_j^J q_j \sum_a^A [E_j^{a,z}(y_a - y_{\text{COM}}^A) - E_j^{a,y}(z_a - z_{\text{COM}}^A)]. \end{aligned}$$

The first and third terms in Eq. (71) cancel each other (pairwise forces/torques on the EFP points and PCM charges). So, Eq. (70) is

$$\begin{aligned} -\tau_{\text{PCM}} &= \sum_j^J q_j \sum_a^A (\partial V_j^a/\partial \theta_a^x) + \sum_j^J q_j \sum_a^A [E_j^{a,z}(y_a - y_{\text{COM}}^A) \\ &\quad - E_j^{a,y}(z_a - z_{\text{COM}}^A)] + \sum_i^I q_i [E_i^{B,z}(y_i - y_{\text{COM}}^A) \\ &\quad - E_i^{B,y}(z_i - z_{\text{COM}}^A)] - \frac{\epsilon}{\epsilon - 1} \\ &\quad \times \sum_i^I \sum_j^J q_i q_j \left[ \frac{z_i - z_j}{|\mathbf{r}_i - \mathbf{r}_j|^3} (y_i - y_{\text{COM}}^A) \right. \\ &\quad \left. - \frac{y_i - y_j}{|\mathbf{r}_i - \mathbf{r}_j|^3} (z_i - z_{\text{COM}}^A) \right]. \end{aligned} \quad (72)$$

The term  $\partial V_j^a/\partial \theta_a^x$  is zero for the EFP charges (monopoles) because the rotation of a point charge leads to no change in its potential, but non-zero for the static dipoles, induced dipoles and static quadrupoles. Equation (72) is similar to Eq. (62), with an additional term for rotations of the EFP multipoles and induced dipoles, and the distances to form the moments (torques). The net torque of an EFP-PCM system calculated with Eq. (72) [based on Eq. (65)] is zero.

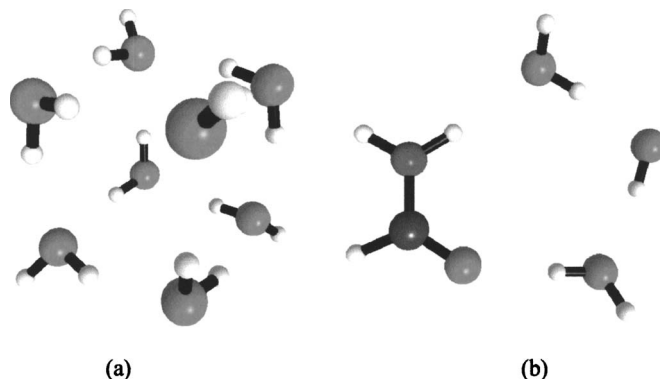


FIG. 1. Two molecular systems: (a) eight EFP1-HF water molecules; (b) QM formamide with three EFP1-HF water molecules.

Both Eqs. (62) and (72) are the VTN approximations to the rigorous expressions that incorporate the derivatives of the areas and positions of the PCM tesserae. A detailed discussion of the VTN approximation can be found in Ref. 17. In a geometry optimization process, the number of PCM tesserae usually varies, thus both the potential energy surface and the gradient surface are usually not continuous. Therefore, rigorous gradients, which are very expensive for large systems, do not necessarily perform better than do approximate ones in PCM geometry optimization. The VTN Eqs. (62) and (72) provide gradients that are within  $\sim 10^{-4}$  a.u. of the exact values and are sufficient for geometry optimizations. The VTN gradients, combined with GEPOL-AS, lead to convergence for almost all geometry optimizations.<sup>17</sup>

### III. NUMERICAL RESULTS AND DISCUSSION

All calculations have been performed with the quantum chemistry program GAMESS,<sup>1,20</sup> in which the codes for the calculation of the QM/EFP/PCM and EFP/PCM energy and gradients are implemented.

Two systems are selected as examples to illustrate geometry optimizations with the gradients calculated using Eqs. (62) and (72). One consists of eight EFP1-HF (Ref. 8) water molecules, which form a cube [Fig. 1(a)]; the other consists of an *ab initio* formamide molecule (restricted Hartree-Fock with a MINI basis set) and three coplanar EFP1-HF water molecules [Fig. 1(b)]. In the C-PCM calculations, spheres with van der Waals radii (H: 1.20 Å, C: 1.70 Å, N: 1.60 Å, and O: 1.50 Å) scaled by the standard factor<sup>6</sup> of 1.20 were used to construct the solute cavity, and no additional spheres were used. The tessellation scheme GEPOL-AS (Ref. 17) was used. The bulk solvent is water with  $\epsilon=78.39$ . The surface charges were solved iteratively without charge renormalization.

The energy and root-mean-square gradient (RMSG) profiles along the geometry optimization course are shown in Fig. 2. In both cases the energies decrease rapidly in the first four steps, as is typically observed in QM geometry optimization calculations for such systems. Then, the energies decrease slowly in the following steps before convergence. In general the RMSG decreases exponentially along the geometry optimization courses (note that the RMSG are plotted in logarithm scale in Fig. 2 to signify the very small changes in

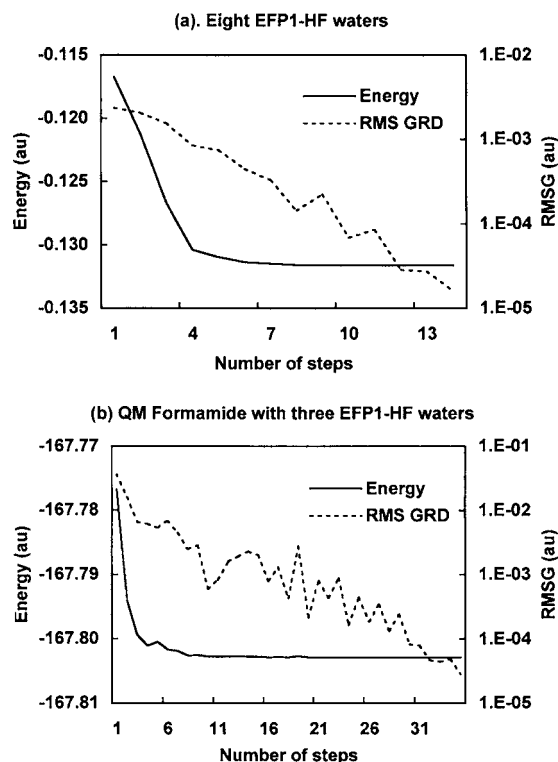


FIG. 2. Energy and root-mean-square gradient (RMSG) profiles in EFP/PCM geometry optimization.

the converging gradients) and falls below  $0.333 \times 10^{-4}$  a.u., the standard GAMESS criterion for the convergence of the RMSG. The criterion for convergence of the maximum gradient is  $1.0 \times 10^{-4}$  a.u. Both cases show that the geometry optimizations can be performed robustly with the approximate gradients described above.

#### IV. CONCLUSION

In combined QM/EFP/PCM calculations the EFP polarization is modeled with LMO dipole polarizability points obtained from *ab initio* calculations, and the PCM bulk polarization is modeled with a set of point charges induced at the molecular surfaces. The EFP polarization and PCM solvation energies in the combined EFP/PCM method are defined and the corresponding energy gradients with respect to molecular geometry changes are derived. All of the energy gradient terms can be expressed as simple electrostatic forces and torques, in accordance with the electrostatic nature of these models. Geometry optimizations can be performed ef-

ficiently with the analytic EFP polarization and PCM solvation energy gradients.

#### ACKNOWLEDGMENTS

This work was supported by a SciDAC (Scientific Discovery through Advanced Computing) grant from the U.S. Department of Energy via the Ames Laboratory.

- <sup>1</sup>M. S. Gordon and M. W. Schmidt, in *Theory and Applications of Computational Chemistry*, edited by C. E. Dykstra, G. Frenking, K. S. Kim, and G. E. Scuseria (Elsevier, New York, 2005).
- <sup>2</sup>J. L. Gao, *Acc. Chem. Res.* **29**, 298 (1996).
- <sup>3</sup>F. J. Vesely, *J. Comput. Phys.* **24**, 361 (1977).
- <sup>4</sup>M. Neumann, F. J. Vesely, O. Steinhauser, and P. Schuster, *Mol. Phys.* **35**, 841 (1978); F. H. Stillinger and C. W. David, *J. Chem. Phys.* **69**, 1473 (1978); P. Barnes, J. L. Finney, J. D. Nicholas, and J. E. Quinn, *Nature (London)* **282**, 459 (1979); A. Warshel, *J. Phys. Chem.* **83**, 1640 (1979).
- <sup>5</sup>F. J. Luque, C. Curutchet, J. Munoz-Muriedas, A. Bidon-Chanal, I. Soteras, A. Morreale, J. L. Gelpi, and M. Orozco, *Phys. Chem. Chem. Phys.* **5**, 3827 (2003); C. J. Cramer and D. G. Truhlar, *Chem. Rev. (Washington, D.C.)* **99**, 2161 (1999); T. N. Truong, *Int. Rev. Phys. Chem.* **17**, 525 (1998).
- <sup>6</sup>J. Tomasi, B. Mennucci, and R. Cammi, *Chem. Rev. (Washington, D.C.)* **105**, 2999 (2005).
- <sup>7</sup>M. S. Gordon, M. A. Freitag, P. Bandyopadhyay, J. H. Jensen, V. Kairys, and W. J. Stevens, *J. Phys. Chem. A* **105**, 293 (2001); I. Adamovic, M. A. Freitag, and M. S. Gordon, *J. Chem. Phys.* **118**, 6725 (2003); I. Adamovic and M. S. Gordon, *Mol. Phys.* **103**, 379 (2005); H. Li and M. S. Gordon, *Theor. Chem. Acc.* **115**, 385 (2006); H. Li, M. S. Gordon, and J. H. Jensen, *J. Chem. Phys.* **124**, 214108 (2006); J. Song and M. S. Gordon (unpublished).
- <sup>8</sup>P. N. Day, J. H. Jensen, M. S. Gordon, S. P. Webb, W. J. Stevens, M. Krauss, D. Garmer, H. Basch, and D. Cohen, *J. Chem. Phys.* **105**, 1968 (1996).
- <sup>9</sup>S. Miertus, E. Scrocco, and J. Tomasi, *Chem. Phys.* **55**, 117 (1981).
- <sup>10</sup>E. Cancès, B. Mennucci, and J. Tomasi, *J. Chem. Phys.* **107**, 3032 (1997).
- <sup>11</sup>V. Barone and M. Cossi, *J. Phys. Chem. A* **102**, 1995 (1998).
- <sup>12</sup>P. Bandyopadhyay, M. S. Gordon, B. Mennucci, and J. Tomasi, *J. Chem. Phys.* **116**, 5023 (2002); H. Li, C. S. Pomelli, and J. H. Jensen, *Theor. Chem. Acc.* **109**, 71 (2003).
- <sup>13</sup>H. Li, H. M. Netzloff, and M. S. Gordon, *J. Chem. Phys.* **125**, (2006).
- <sup>14</sup>R. S. Varga, *Matrix Iterative Analysis*, 2nd ed. (Springer, New York, 2000).
- <sup>15</sup>A. R. Leach, *Molecular Modelling: Principles and Applications*, 2nd ed. (Prentice-Hall, Harlow, 2001).
- <sup>16</sup>M. Cossi, N. Rega, G. Scalmani, and V. Barone, *J. Comput. Chem.* **24**, 669 (2003).
- <sup>17</sup>H. Li and J. H. Jensen, *J. Comput. Chem.* **25**, 1449 (2004).
- <sup>18</sup>J. L. Pascualahir, E. Silla, and I. Tunon, *J. Comput. Chem.* **15**, 1127 (1994); E. Silla, I. Tunon, and J. L. Pascualahir, *ibid.* **12**, 1077 (1991); E. Silla, F. Villar, O. Nilsson, J. L. Pascualahir, and O. Tapia, *J. Mol. Graphics* **8**, 168 (1990); J. L. Pascualahir and E. Silla, *J. Comput. Chem.* **11**, 1047 (1990).
- <sup>19</sup>E. Cancès, B. Mennucci, and J. Tomasi, *J. Chem. Phys.* **109**, 260 (1998); E. Cancès and B. Mennucci, *ibid.* **109**, 249 (1998).
- <sup>20</sup>M. W. Schmidt, K. K. Baldrige, J. A. Boatz *et al.*, *J. Comput. Chem.* **14**, 1347 (1993).